

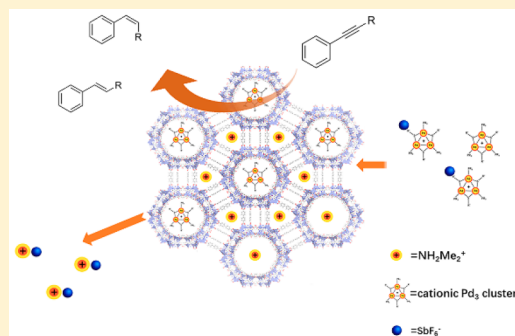
Heterogenization of Trinuclear Palladium Complex into an Anionic Metal–Organic Framework through Postsynthetic Cation Exchange

Junyu Ren, Pui Ching Lan, Meng Chen, Weijie Zhang, and Shengqian Ma*[ⓑ]

Department of Chemistry, University of South Florida, 4202 East Fowler Avenue, Tampa, Florida 33620, United States

S Supporting Information

ABSTRACT: The innate modular nature of metal–organic frameworks (MOFs) enables postsynthetic modification of the crystalline framework, thereby resulting in novel properties. Anionic MOFs are an interesting category of frameworks since their pore environment can be modified using a simple ion-exchange process. In this work, we demonstrate that via directly ion exchanging an anionic metal–organic framework can not only be the host for a palladium trinuclear transition metal complex but also gain catalytic capability as a hybrid system in the semireduction of internal alkynes. The confined pore space within the MOF structure and the thiol groups of the cluster successfully minimize the detrimental aggregation of palladium during the catalytic process, thereby resulting in a heterogeneous recyclable catalyst system.



INTRODUCTION

Much attention has been focused on the heterogenization of homogeneous catalyst on solid supports in past decade, due to their integration showing the potential to combine the advantages of both homogeneous and heterogeneous catalysis.^{1,2} Loading onto supports could prevent the metal atoms or small clusters from aggregating, which leads to catalyst deactivation. Activated carbon, zeolites, and organic polymers are the three most popular hosts for the molecular catalyst and result in numerous efficient and recyclable catalyst systems.³ However, most of these are amorphous materials, and it is difficult to decipher the structure–property relationships as well as host–guest interactions.⁴

As an emerging class of porous materials with high crystallinity nature, metal–organic frameworks (MOFs) feature great amenability to design, high surface areas, tunable pore sizes, and tailorable functionality, and this class has long been proposed as a host for the heterogenization of homogeneous catalysts.^{5,6} Catalyst@MOFs hybrids inherit the features of active and selective catalytic sites, programmable chemical environment, and easy postreaction separation from the parent constituents. In addition, metal–support interactions are well-known to isolate the active centers and prevent them from aggregating, by which means the catalytically active centers could be isolated within the pore space and thus decrease multimetallic decomposition.^{7,8} Direct encapsulation without covalent interaction is one common strategy for heterogenization.⁹ Either MOFs are built around the catalysts (bottle-around-ship strategy), or molecular catalysts are synthesized *in situ* and limited inside the framework (ship-in-the-bottle strategy). An alternative method was first reported by encapsulating cationic catalysts into anionic cages.¹⁰ Sanford's group then presented the incorporation of cationic

complexes into MOFs (ZJU-28 and MIL-101-SO₃) via cation exchanging.¹¹ Subsequently, Rosseinsky and co-workers presented a recyclable heterogeneous [catalyst]⁺@[MOF][−] system for a Diels–Alder catalyst.¹² This approach avoids covalent tethering which requires intense synthesis that has deleteriously affects to the catalytic system. Besides, complexes were partially immobilized via complementary electrostatic interaction instead of fully depending on the size limitations. Although the above-mentioned MOF-supported catalytic species have been developed, research on multinuclear complex encapsulation in MOFs is still limited.

Compared with the single-site transition metal catalysts, trinuclear metal–aromatic complexes are an interesting category of material in catalytic field.¹³ They are metal analogues of the cyclopropenyl cation, with their all-metal aromaticity involving d-type atomic orbitals. Among the transition metal family, palladium is a good candidate to generate aromatic bonding patterns involving unfilled d orbitals. The triangles are formed by three Pd atoms, with three identical 60° angles and the same metal–metal bonds. The coexistence of thiol groups and phosphines stabilizes the Pd core while leaving metal sites accessible for substrates. Palladiums and heteroatoms were nearly coplanar (largest dihedral angles remaining below 2°). The phosphines on the palladium centers point in the same direction, and sulfur substituents point in the opposite direction, with a perfect alternation (Figures S1 and S2). With a positively charged metal core, they act as a Lewis acid, while the delocalized

Special Issue: Organometallic Chemistry within Metal–Organic Frameworks

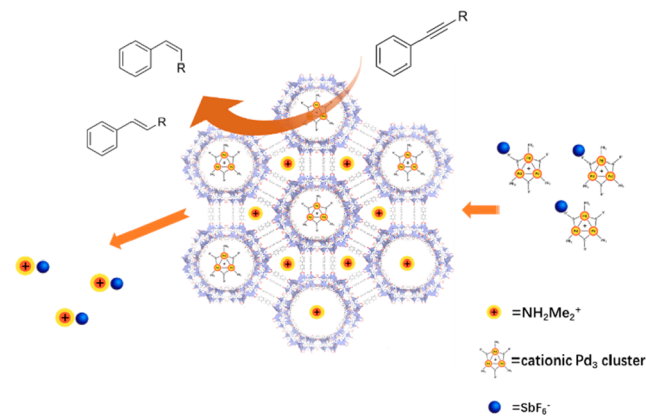
Received: April 30, 2019

HOMO contributes Lewis basic properties to the triangular core. In comparison with the mononuclear complexes, they show more bonding modes and different mechanism as catalysts.¹⁴

Research on new catalytic species for the semihydrogenation of acetylene to ethylene is the subject of present research interest.¹⁵ The reaction is widely applied in industry, particularly in the case of industrial polymerization of ethylene to polyethylene to purify the feedstock from acetylene, which would otherwise poison the polymerization catalyst.¹⁶ Transfer hydrogenation (TH) reaction, referring to the addition of hydrogen to a molecule from a non-H₂ hydrogen source, is becoming the center of research to access various hydrogenated compounds, mainly due to (i) no need for hazardous pressurized H₂ gas or elaborate experimental setups, (ii) easy handling of the hydrogen donors, and (iii) ready accessibility of the catalysts that are involved.¹⁷

For noble-metal–aromatic clusters, heterogenization would enable separation and recyclability which has a profound significance in industry. In this work, we report the encapsulation of two trinuclear cationic palladium clusters (Pd₃ cluster-1 and Pd₃ cluster-2, Supporting Information, Section S3) inside the pores of the anionic metal–organic framework bio-MOF 100 (Scheme 1), generating bio-MOF

Scheme 1. Illustrative Scheme of the Encapsulation of Palladium Cluster within bio-MOF 100 for Heterogeneous Chemo-Selective Semireduction of Internal Alkynes



100-1 and bio-MOF 100-2. Catalytic performance parameters regarding stability, activity, and product selectivity were evaluated for the title sample. The catalytic activity of the cluster@MOF system is comparable to that of the homogeneous counterpart. It is also interesting to observe that the catalytic behavior of the trinuclear palladium cluster was altered after encapsulated into the confined MOF structure. This strategy liberates the metal catalyst and the MOF from intense synthetic modification. The obtained cluster@MOF complexes are proven to be heterogeneous recyclable catalysts for the semihydrogenation of alkynes.

RESULTS AND DISCUSSION

Encapsulation via Cation Exchange. First, cation-exchange experiments were performed to replace the original counterion H₂NMe₂⁺. Bio-MOF 100 crystals were soaked into CHCl₃ solutions of Pd₃ complexes for 1 week to ensure certain degree of cation exchange. Transparent crystals were found to transform to a deep color, while the solvents' color turned to a

lighter red. Fresh stock solution was added several times until a comprehensive color change of the crystals was observed under microscope (Figure 1). Optical microscopy of the cross section

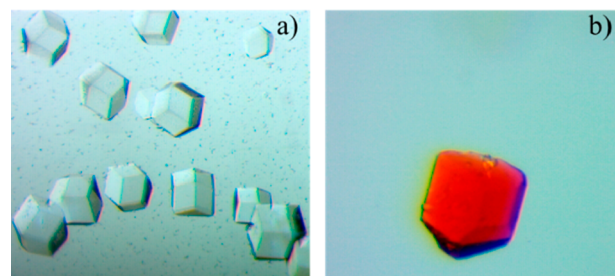


Figure 1. Optical microscopy images of (a) bio-MOF 100 and (b) bio-MOF 100-1.

(Figure S4) showed Pd₃ complexes spreading across the whole crystal rather than just the periphery of crystal. Through ICP-mass spectrometry (MS) analysis, the Pd/Zn ratio was measured after digestion in diluted HCl, by which the exchange result was further confirmed. Results showed the Pd contents are, respectively, 5.16 and 6.40 wt % in the bio-MOF 100-1 and bio-MOF 100-2 complexes with 15.2 and 14% of the H₂NMe₂⁺ counterion being replaced. From the aspect of the charge balance, one complex replaces one H₂NMe₂⁺. However, if the size differences between Pd cluster and H₂NMe₂⁺ were considered, then the upper limit for the replacement is about 15%, because the diameter of the complex (~16 Å) is bigger than the H₂NMe₂⁺ cations (~3 Å), as the ICP-MS data proved.

NMR spectroscopy was also applied to verify the incorporation of the Pd₃ cation in anionic framework by digesting Pd₃@bio-MOF 100 complex in DCl/dms-*d*₆ (Figure 2). Since the Pd₃ cation is too stable for the digestion

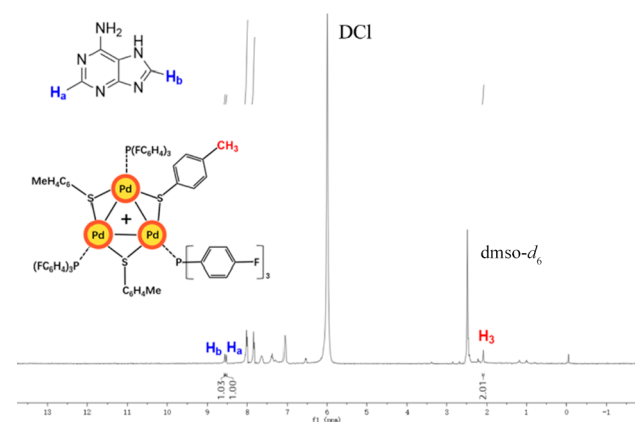


Figure 2. ¹H NMR spectrum of bio-MOF 100-1 digested in DCl/dms-*d*₆.

conditions, a holistic analysis of the encapsulated guests were performed to analyze the postencapsulation complex. Quantitative study of cation exchange was done through comparing integrations of relative peak areas from the pyridine ring of adenine (8.52 ppm, 1H) and methyl group on cluster (2.09 ppm, 9H). For bio-MOF 100-1 and bio-MOF 100-2, the replacement ratio was determined to be 22 and 21% according to the formula of bio-MOF 100 (Zn₈(ad)₄(BPDC)₆O₂·4Me₂NH₂). The encapsulation ratios determined by NMR

spectrum differ from the ICP-MS data, which could be attributed to the strength of the cluster. It did not completely decompose, and part of it was filtered together with the organic ligand before the ICP-MS test.

Comparison of PXRD patterns of Pd₃@MOF with pure bio-MOF 100 reveals that the structure remains intact after the cation-exchanging process (Figure 3). Also, it shows that the

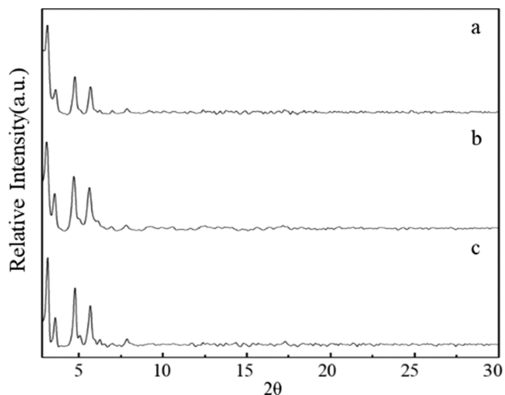


Figure 3. PXRD patterns of (a) bio-MOF 100, (b) bio-MOF 100-1, and (c) bio-MOF 100-2.

Pd₃@MOF material could retain its structure after storing for a long time. The N₂ sorption studies (Figure 4) showed that in

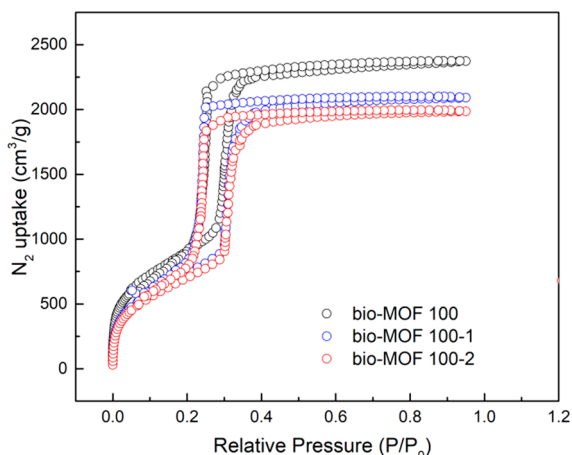


Figure 4. N₂ sorption isotherms at 77 K of bio-MOF 100, bio-MOF 100-1, and bio-MOF 100-2.

comparison with bio-MOF 100 a decrease in the Brunauer–Emmett–Teller surface area (from 3115 to 2793/2646 m² g⁻¹) was observed because of the incorporation of the Pd₃ cluster.

Semireduction of Internal Alkynes. Selective hydrogenation of alkynes to alkenes, instead of alkane, is of cardinal significance in industry.¹⁸ It is indispensable in the petrochemical industry and the manufacture of pharmaceuticals and fine chemicals. However, selective hydrogenations with discrimination between alkenes and alkanes are very challenging. With the palladium core being partially poisoned by thiol groups, trinuclear palladium clusters are good candidates for the selective hydrogenation reaction. In this contribution, bio-MOF 100-1 and bio-MOF 100-2 were studied for the semireduction of internal alkynes. The yield and selectivity were calculated according to the integration ratio of ¹H NMR spectra. As expected, the control experiment

(Table 1, entry 1) indicates that bio-MOF 100 does not catalyze this reaction. Under standard reaction conditions

Table 1. Investigation of bio-MOF 100-1 and bio-MOF 100-2 in the Semireduction of Internal Alkynes^a

entry	substrate	catalyst	t (h)	conversion ^b	selectivity ^b
1	a and b	bio-MOF 100	96	0%	
2	a	bio-MOF 100-1	96	95%	95%
3	a	bio-MOF 100-2	48	94%	94%
4	b	bio-MOF 100-1	36	91%	94%
5	b	bio-MOF 100-2	36	89%	96%
6	a	Pd complex-1	96	88%	92%
		Pd complex-2	10	90%	90%
7	b	Pd complex-1	10	95%	98%
		Pd complex-2	10	96%	99%

^aReaction conditions: 30 mg Pd₃@bio-MOF 100 catalyst, 45 μL formic acid(1.2 mmol), 167 μL triethylamine(1.2 mmol), 3.5 mL THF, 70 °C. ^bDetermined by ¹H NMR.

(Table 1, entry 2), the model reaction using 1-phenylpropyne as substrate, 5.16 wt % bio-MOF 100-1 (5.16 wt % based on Pd content) as the catalyst, and HCO₂H/NEt₃ as the hydrogen source, gave 95% yield in THF after heating at 70 °C for 96 h. The product shows good Z selectivity (95%) together with (E)-phenylpropene (5%) (determined by ¹H NMR, Figure S8). Then, the substrate was extended to diaryl-substituted acetylenes (substrate b). A conversion rate of 91% was achieved by bio-MOF 100-1 to the product with 94% selectivity toward [Z]-stilbene (Table 1, entry 4). Compared with the homogeneous counterpart, the Pd₃@MOF system shows variations for catalytic behavior, which could be attributed to the long-range chemical environment surrounding the metal clusters. The adsorption and binding behavior of substrates on the metal site could be altered after encapsulating the palladium complex into a confined space. Last, the alkane was not observed even prolonging the heating time for another 24 h.

Recycling experiments were performed (Figure 5) and show that bio-MOF 100-1 could be recycled 2 times with 74% yield for the second cycle and 69% for the third cycle (determined by ¹H NMR, Figures S9 and S10). For bio-MOF 100-2, it was observed that the second and third recycling percents are 72 and 64%, respectively (Figures S12 and S13). The products showed Z-preferred selectivity in all recycling experiments. From the PXRD patterns, it was observed that the overall structure of the MOF did not change after 3 catalytic cycles. Compared with the homogeneous counterparts, the Pd₃@MOF version shows the ability as heterogeneous catalyst which can be recovered from the liquid phase while retaining respectable catalytic activity. The decrease of catalytic activity could attribute to slowly decomposition of metal complexes, as already been noted in homogeneous catalysis where the loss of activity is more pronounced. Besides, defects formed inside the framework could also bring a negative effect to the catalytic system.

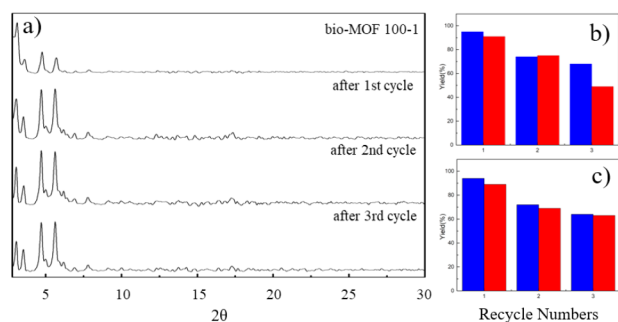


Figure 5. PXRD patterns of (a) bio-MOF 100-1 after each reaction cycles. (b) Recycling performances of bio-MOF 100-1. Blue columns = 1-phenylpropyne as substrate, red columns = diphenylethyne as substrate. (c) Recycling performances of bio-MOF 100-2. Blue columns = 1-phenylpropyne as substrate, red columns = diphenylethyne as substrate.

Leaching tests were performed as described in the [Experimental Section](#). It was proven that the reaction did not proceed after the removal of Pd₃@MOF catalyst. In the catalytic reactions, a HCO₂H/NEt₃ stock solution was made in advance, and the pH was carefully maintained at 7 to minimize the potential detrimental effect to the MOF structure as well as the encapsulated Pd₃ cluster.

CONCLUSION

In summary, we demonstrated the successful incorporation of two trinuclear palladium complexes into the anionic MOF, bio-MOF 100, through a direct cation-exchanging method. Electrostatic interaction between the cation complex and the anionic framework stabilizes the palladium complex through Coulombic force, thereby rendering it with good recyclability as well as respectable catalytic activity for the semireduction of internal alkynes. The obtained complexes are proven to be heterogeneous recyclable catalysts for the semihydrogenation of alkynes, which cannot be achieved for their homogeneous counterparts. Moreover, the thiol groups of the cluster and the confined pore space within the MOF minimize the detrimental aggregation of palladium during the catalytic process. Further studies in our lab will aim to design heterogeneous catalytic systems based on a MOF platform for other types of chemoselective catalysis and to gain a better understanding of the mechanisms.

EXPERIMENTAL SECTION

Preparation of bio-MOF 100 and Pd₃ Cluster Catalyst.

Material bio-MOF 100 was synthesized according to the method described in previous work with little modulation.¹⁹ In brief, Zn(NO₃)₂·6H₂O (0.05M, 7.5 mL), adenine (0.05M, 2.5 mL), H₂BPDC (0.1M, 2 mL), H₃-BTB (0.1M, 0.5 mL), HNO₃ (1M, 600 μL), and 1 mL of H₂O were mixed and divided into 7 Pyrex tubes. Then, the tubes were sealed on a Schlenk line and heated in a 135 °C oven for 24 h. The as-obtained crystals were washed with fresh DMF and put into a 100 °C oven for another 24 h to get rid of most of the uncoordinated ligand. Pd₃ clusters were synthesized completely according to previous work.

Synthesis of Trinuclear Palladium Cluster. In a N₂-filled glovebox, Pd(dba)₂ (115 mg, 0.2 mmol) was completely dissolved in CHCl₃ (20 mL). Then, phosphine (0.2 mmol, 63 mg for tris(4-fluorophenyl) phosphine, 61 mg for tris(4-methylphenyl) phosphine) and disulfide (0.1 mmol, 25 mg for *p*-tolyl disulfide and 10 mg for methyl disulfide) were added also under nitrogen atmosphere. The resulting mixture was stirred at room temperature for 4 h. Silver

hexafluoroantimonate (0.067 mmol, 23 mg) was then introduced into the mixture and stirred for an additional 1 h. The deep red mixture was filtered by a 0.45 μm syringe membrane filter, and the solvent was removed under vacuum. Raw product was washed three times by CH₂Cl₂/*n*-hexane (1:30 v/v) mixture to remove impurities. Last, the pure cluster was dried under vacuum. The purity of the complex was characterized by ¹H NMR spectra in CDCl₃.

Preparation of Pd₃@bio-MOF 100 Catalyst. In a 10 mL scintillation vial, bio-MOF 100 crystals were soaked in CHCl₃ (5 mL). Then, a solution of Pd₃ cluster in CHCl₃ (0.01 M, 5 mL) was added into the MOF suspension. The solution was changed every day within 1 week. At the end, the crystals were washed with fresh CHCl₃ (4 × 10 mL). The as-obtained Pd₃@MOF was then stored in CHCl₃ solution for further use.

General Procedure for Semireduction of Internal Alkynes.

The Pd₃@MOF (30 mg, 0.0048 mmol) was put into a 25 mL Schlenk tube equipped with a small magnetic stir bar. A HCO₂H/NEt₃ stock solution in THF (HCO₂H/NEt₃ = 1:1, 4 equiv, 3.5 mL) was then added to the tube, and substrates (0.3 mmol, 1 equiv) were added to the tube after 10 min. The Schlenk tube was capped and taken out of the glovebox and heated in an oil bath for the noted time. The catalyst was separated by centrifugation. The product was isolated as indicated in the [Supporting Information](#).

Characterization of the Pd₃@bio-MOF 100 Catalysts. Powder X-ray diffraction (PXRD) was performed on a Bruker AXS X-ray diffractometer. Cu Kα radiation of 40 mA, 40 kV, K₁ = 0.15418 nm, 2θ scanning range of 2–40°, a scan step size of 0.02°, and a time of 3 s per step. The samples were ground to smaller particles and placed on a zero-background silicon holder. Brunauer–Emmett–Teller surface areas were determined by N₂ adsorption/desorption isotherms at 77 K using automatic volumetric adsorption equipment (Micromeritics ASAP2020). Pretreatment was done by using super critical CO₂ method. Digestion analysis was performed by ¹H NMR, approximately 3 mg of dried MOF material was digested with sonication in 600 μL of DMSO-*d*₆ and 10 μL of DCl. The NMR tests were performed on a Varian Unity Inova 400 spectrometer.

Recycling Experiments. The reaction mixture was centrifuged after the reaction, and the liquid layer was siphoned out. The residual solid was then washed with THF solution and centrifuged. This process was repeated twice followed by drying of the solid in nitrogen flow. The HCO₂H/NEt₃ stock solution in THF and substrate were then added to the glovebox for the next reaction cycle.

Pd₃@bio-MOF 100 Catalyst Leaching Test. In a 25 mL Schlenk tube, the Pd₃@MOF (30 mg), HCO₂H/NEt₃ stock solution in THF, and substrate were added. The tube was then taken out of glovebox and heated at 70 °C. After 12 h, the reaction was cooled to room temperature. In the glovebox, the solution was filtered. Half of the filtrate was removed and dried for NMR analysis. The remaining solution was transferred to another 25 mL Schlenk tube and heated at 70 °C for another 36 h. Then, the yield was again determined via NMR. The result shows that the reaction did not go any further after Pd₃@MOF was removed.

ASSOCIATED CONTENT

Supporting Information

The Supporting Information is available free of charge on the [ACS Publications website](#) at DOI: [10.1021/acs.organomet.9b00286](https://doi.org/10.1021/acs.organomet.9b00286).

Synthetic procedures of related compounds; SEM images; ¹H NMR spectra of related compounds (PDF)

AUTHOR INFORMATION

Corresponding Author

*E-mail: sqma@usf.edu.

ORCID

Shengqian Ma: 0000-0002-1897-7069

Notes

The authors declare no competing financial interest.

ACKNOWLEDGMENTS

We acknowledge the NSF (DMR-1352065) and the University of South Florida for financial support of this work.

REFERENCES

- (1) (a) Madhavan, N.; Jones, C. W.; Weck, M. Rational approach to polymer-supported catalysts: synergy between catalytic reaction mechanism and polymer design. *Acc. Chem. Res.* **2008**, *41*, 1153–1165. (b) Baleizao, C.; Garcia, H. Chiral salen complexes: an overview to recoverable and reusable homogeneous and heterogeneous catalysts. *Chem. Rev.* **2006**, *106*, 3987–4043. (c) Ye, R.; Zhukhovitskiy, A. V.; Deraedt, C. V.; Toste, F. D.; Somorjai, G. A. Supported dendrimer-encapsulated metal clusters: toward heterogenizing homogeneous catalysts. *Acc. Chem. Res.* **2017**, *50*, 1894–1901.
- (2) (a) Trzeciak, A. M.; Ziolkowski, J. J. Monomolecular, nanosized and heterogenized palladium catalysts for the Heck reaction. *Coord. Chem. Rev.* **2007**, *251*, 1281–1293. (b) Wang, Z.; Chen, G.; Ding, K. Self-supported catalysts. *Chem. Rev.* **2009**, *109*, 322–359. (c) Jain, K. R.; Herrmann, W. A.; Kühn, F. E. Synthesis and catalytic applications of chiral monomeric organomolybdenum (VI) and organorhenium (VII) oxides in homogeneous and heterogeneous phase. *Coord. Chem. Rev.* **2008**, *252*, 556–568. (d) Lu, J.; Toy, P. H. Organic polymer supports for synthesis and for reagent and catalyst immobilization. *Chem. Rev.* **2009**, *109*, 815–838.
- (3) (a) Westerhaus, F. A.; Jagadeesh, R. V.; Wienhofer, G.; Pohl, M.-M.; Radnik, J.; Surkus, A.-E.; Rabeah, J.; Junge, K.; Junge, H.; Nielsen, M.; et al. Heterogenized cobalt oxide catalysts for nitroarene reduction by pyrolysis of molecularly defined complexes. *Nat. Chem.* **2013**, *5*, 537–543. (b) Ganga, V. S. R.; Dabbawala, A. A.; Munusamy, K.; Abdi, S. H.; Kureshy, R. I.; Khan, N. H.; Bajaj, H. C. Rhodium complexes supported on nanoporous activated carbon for selective hydroformylation of olefins. *Catal. Commun.* **2016**, *84*, 21–24. (c) Gogoi, P.; Dutta, A. K.; Saikia, S.; Borah, R. Heterogenized hybrid catalyst of 1-sulfonic acid-3-methyl imidazolium ferric chloride over NaY zeolite for one-pot synthesis of 2-amino-4-arylpyrimidine derivatives: A viable approach. *Appl. Catal., A* **2016**, *523*, 321–331. (d) Yang, H.; Luo, M.; Luo, L.; Wang, H.; Hu, D.; Lin, J.; Wang, X.; Wang, Y.; Wang, S.; Bu, X.; Feng, P.; Wu, T. Highly selective and rapid uptake of radionuclide cesium based on robust zeolitic chalcogenide via stepwise ion-exchange strategy. *Chem. Mater.* **2016**, *28*, 8774–8780. (e) Ratnasamy, P.; Srinivas, D. Selective oxidations over zeolite-and mesoporous silica-based catalysts: Selected examples. *Catal. Today* **2009**, *141*, 3–11. (f) Ishida, T.; Nagaoka, M.; Akita, T.; Haruta, M. Deposition of gold clusters on porous coordination polymers by solid grinding and their catalytic activity in aerobic oxidation of alcohols. *Chem. - Eur. J.* **2008**, *14*, 8456–8460.
- (4) (a) Lemus-Yegres, L. J.; Such-Basáñez, I.; Román-Martínez, M. C.; De Lecea, C. S. M. Catalytic properties of a Rh-diamine complex anchored on activated carbon: Effect of different surface oxygen groups. *Appl. Catal., A* **2007**, *331*, 26–33. (b) Mignoni, M. L.; de Souza, M. O.; Pergher, S. B.; de Souza, R. F.; Bernardo-Gusmão, K. Nickel oligomerization catalysts heterogenized on zeolites obtained using ionic liquids as templates. *Appl. Catal., A* **2010**, *374*, 26–30. (c) Zhang, Y.; Riduan, S. N. Functional porous organic polymers for heterogeneous catalysis. *Chem. Soc. Rev.* **2012**, *41*, 2083–2094.
- (5) (a) Chen, L.; Chen, H.; Luque, R.; Li, Y. Metal-organic framework encapsulated Pd nanoparticles: Towards advanced heterogeneous catalysts. *Chem. Sci.* **2014**, *5*, 3708–3714. (b) Lu, G.; Li, S.; Guo, Z.; Farha, O. K.; Hauser, B. G.; Qi, X.; Wang, Y.; Wang, X.; Han, S.; Liu, X.; et al. Imparting functionality to a metal-organic framework material by controlled nanoparticle encapsulation. *Nat. Chem.* **2012**, *4*, 310–316. (c) Zhang, Y.; Degirmenci, V.; Li, C.; Hensen, E. J. Phosphotungstic acid encapsulated in metal-organic framework as catalysts for carbohydrate dehydration to 5-hydroxymethylfurfural. *ChemSusChem* **2011**, *4*, 59–64. (d) Janssens, N.; Wee, L. H.; Bajpe, S.; Breynaert, E.; Kirschhock, C. E.; Martens, J. A. Recovery and reuse of heteropolyacid catalyst in liquid reaction medium through reversible encapsulation in $\text{Cu}_3(\text{BTC})_2$ metal-organic framework. *Chem. Sci.* **2012**, *3*, 1847–1850.
- (6) (a) Drout, R. J.; Robison, L.; Farha, O. K. Coordin. Catalytic applications of enzymes encapsulated in metal-organic frameworks. *Coord. Chem. Rev.* **2019**, *381*, 151–160. (b) Dhakshinamoorthy, A.; Asiri, A. M.; Garcia, H. Formation of C-C and C-Heteroatom Bonds by C-H Activation by Metal Organic Frameworks as Catalysts or Supports. *ACS Catal.* **2019**, *9* (2), 1081–1102. (c) Liang, J.; Huang, Y. B.; Cao, R. Coordin. Metal-organic frameworks and porous organic polymers for sustainable fixation of carbon dioxide into cyclic carbonates. *Coord. Chem. Rev.* **2019**, *378*, 32–65. (d) Kirchon, A.; Feng, L.; Drake, H. F.; Joseph, E. A.; Zhou, H. C. From fundamentals to applications: a toolbox for robust and multifunctional MOF materials. *Chem. Soc. Rev.* **2018**, *47*, 8611–8638. (e) Li, G.; Zhao, S.; Zhang, Y.; Tang, Z. Metal-Organic Frameworks Encapsulating Active Nanoparticles as Emerging Composites for Catalysis: Recent Progress and Perspectives. *Adv. Mater.* **2018**, *30*, 1800702. (f) Drake, T.; Ji, P.; Lin, W. Site Isolation in Metal-Organic Frameworks Enables Novel Transition Metal Catalysis. *Acc. Chem. Res.* **2018**, *51*, 2129–2138. (g) Liu, J.; Chen, L.; Cui, H.; Zhang, J.; Zhang, L.; Su, C.-Y. Applications of metal-organic frameworks in heterogeneous supramolecular catalysis. *Chem. Soc. Rev.* **2014**, *43*, 6011–6061. (h) Gu, Z.-Y.; Park, J.; Raiff, A.; Wei, Z.; Zhou, H.-C. Metal-organic frameworks as biomimetic catalysts. *ChemCatChem* **2014**, *6*, 67–75. (i) Aguila, B.; Sun, Q.; Wang, X.; O'Rourke, E.; Al-Enizi, A. M.; Nafady, A.; Ma, S. Lower Activation Energy for Catalytic Reactions through Host-Guest Cooperation within Metal-Organic Frameworks. *Angew. Chem., Int. Ed.* **2018**, *57*, 10107–10111.
- (7) (a) Li, Z.; Schweitzer, N. M.; League, A. B.; Bernales, V.; Peters, A. W.; Getsoian, A. B.; Wang, T. C.; Miller, J. T.; Vjunov, A.; Fulton, J. L.; et al. Sintering-resistant single-site nickel catalyst supported by metal-organic framework. *J. Am. Chem. Soc.* **2016**, *138*, 1977–1982. (b) Zhao, M.; Yuan, K.; Wang, Y.; Li, G.; Guo, J.; Gu, L.; Hu, W.; Zhao, H.; Tang, Z. Metal-organic frameworks as selectivity regulators for hydrogenation reactions. *Nature* **2016**, *539*, 76–80.
- (8) Xiao, D. J.; Oktawiec, J.; Milner, P. J.; Long, J. R. Pore Environment Effects on Catalytic Cyclohexane Oxidation in Expanded $\text{Fe}_2(\text{dobdc})$ Analogues. *J. Am. Chem. Soc.* **2016**, *138*, 14371–14379.
- (9) Li, B.; Zhang, Y.; Ma, D.; Ma, T.; Shi, Z.; Ma, S. Metal-Cation-Directed de Novo Assembly of a Functionalized Guest Molecule in the Nanospace of a Metal-Organic Framework. *J. Am. Chem. Soc.* **2014**, *136*, 1202–1205.
- (10) (a) Brown, C. J.; Miller, G. M.; Johnson, M. W.; Bergman, R. G.; Raymond, K. N. High-turnover supramolecular catalysis by a protected ruthenium (II) complex in aqueous solution. *J. Am. Chem. Soc.* **2011**, *133*, 11964–11966. (b) Wang, Z. J.; Brown, C. J.; Bergman, R. G.; Raymond, K. N.; Toste, F. D. Hydroalkoxylation catalyzed by a gold (I) complex encapsulated in a supramolecular host. *J. Am. Chem. Soc.* **2011**, *133*, 7358–7360. (c) Wang, Z. J.; Clary, K. N.; Bergman, R. G.; Raymond, K. N.; Toste, F. D. A supramolecular approach to combining enzymatic and transition metal catalysis. *Nat. Chem.* **2013**, *5*, 100.
- (11) (a) Genna, D. T.; Wong-Foy, A. G.; Matzger, A. J.; Sanford, M. S. Heterogenization of homogeneous catalysts in metal-organic frameworks via cation exchange. *J. Am. Chem. Soc.* **2013**, *135*, 10586–10589. (b) Genna, D. T.; Pfund, L. Y.; Samblanet, D. C.; Wong-Foy, A. G.; Matzger, A. J.; Sanford, M. S. Rhodium hydrogenation catalysts supported in metal organic frameworks: influence of the framework on catalytic activity and selectivity. *ACS Catal.* **2016**, *6*, 3569–3574.
- (12) Grigoropoulos, A.; Whitehead, G. F. S.; Perret, N.; Katsoulidis, A. P.; Chadwick, F. M.; Davies, R. P.; Haynes, A.; Brammer, L.; Weller, A. S.; Xiao, J.; Rosseinsky, M. J. Encapsulation of an organometallic cationic catalyst by direct exchange into an anionic MOF. *Chem. Sci.* **2016**, *7*, 2037–2050.

- (13) (a) Deyris, P. A.; Cañeque, T.; Wang, Y.; Retaillieu, P.; Bigi, F.; Maggi, R.; Maestri, G.; Malacria, M. Catalytic Semireduction of Internal Alkynes with All-Metal Aromatic Complexes. *ChemCatChem* **2015**, *7*, 3266–3269. (b) Monfredini, A.; Santacroce, V.; Marchiò, L.; Maggi, R.; Bigi, F.; Maestri, G.; Malacria, M. Semi-Reduction of internal alkynes with prototypical subnanometric metal surfaces: bridging homogeneous and heterogeneous catalysis with trinuclear all-metal aromatics. *ACS Sustainable Chem. Eng.* **2017**, *5*, 8205–8212. (c) Lanzi, M.; Cañeque, T.; Marchiò, L.; Maggi, R.; Bigi, F.; Malacria, M.; Maestri, G. Alternative Routes to Tricyclic Cyclohexenes with Trinuclear Palladium Complexes. *ACS Catal.* **2018**, *8*, 144–147.
- (14) (a) Blanchard, S.; Fensterbank, L.; Gontard, G.; Lacôte, E.; Maestri, G.; Malacria, M. Synthesis of Triangular Tripalladium Cations as Noble-Metal Analogues of the Cyclopropenyl Cation. *Angew. Chem., Int. Ed.* **2014**, *53*, 1987–1991. (b) Wang, Y.; Monfredini, A.; Deyris, P. A.; Blanchard, F.; Derat, E.; Maestri, G.; Malacria, M. All-metal aromatic cationic palladium triangles can mimic aromatic donor ligands with Lewis acidic cations. *Chem. Sci.* **2017**, *8*, 7394–7402.
- (15) (a) Armbrüster, M.; Kovnir, K.; Behrens, M.; Teschner, D.; Grin, Y.; Schlögl, R. Pd-Ga intermetallic compounds as highly selective semihydrogenation catalysts. *J. Am. Chem. Soc.* **2010**, *132*, 14745–14747. (b) Ota, A.; Armbrüster, M.; Behrens, M.; Rosenthal, D.; Friedrich, M.; Kasatkin, I.; Girgsdies, F.; Zhang, W.; Wagner, R.; Schlögl, R. Intermetallic compound Pd₂Ga as a selective catalyst for the semi-hydrogenation of acetylene: from model to high performance systems. *J. Phys. Chem. C* **2011**, *115*, 1368–1374. (c) Xu, X.; Kehr, G.; Daniliuc, C. G.; Erker, G. Stoichiometric Reactions and Catalytic Hydrogenation with a Reactive Intramolecular Zr⁺/Amine Frustrated Lewis Pair. *J. Am. Chem. Soc.* **2015**, *137*, 4550. (d) Welch, G. C.; Juan, R. R. S.; Masuda, J. D.; Stephan, D. W. Reversible, metal-free hydrogen activation. *Science* **2006**, *314*, 1124–1126. (e) Niu, Z.; Bhagya Gunatilleke, W. D.C.; Sun, Q.; Lan, P. C.; Perman, J.; Ma, J.-G.; Cheng, Y.; Aguila, B.; Ma, S. Metal-organic framework anchored with a Lewis pair as a new paradigm for catalysis. *Chem* **2018**, *4*, 2587–2599. (f) Niu, Z.; Zhang, W.; Lan, P. C.; Aguila, B.; Ma, S. Promoting Frustrated Lewis Pair for Heterogeneous Chemoselective Hydrogenation via Tailored Pore Environment within Metal-Organic Framework. *Angew. Chem., Int. Ed.* **2019**, *58*, 7420–7424.
- (16) (a) Borodziński, A.; Bond, G. C. Selective hydrogenation of ethyne in ethene-rich streams on palladium catalysts. Part 1. Effect of changes to the catalyst during reaction. *Catal. Rev.: Sci. Eng.* **2006**, *48*, 91–144. (b) Borodziński, A.; Bond, G. C. Selective hydrogenation of ethyne in ethene-rich streams on palladium catalysts, Part 2: Steady-state kinetics and effects of palladium particle size, carbon monoxide, and promoters. *Catal. Rev.: Sci. Eng.* **2008**, *50*, 379–469.
- (17) (a) Wang, D.; Astruc, D. The golden age of transfer hydrogenation. *Chem. Rev.* **2015**, *115*, 6621–6686. (b) Chinchilla, R.; Najera, C. Chemicals from alkynes with palladium catalysts. *Chem. Rev.* **2014**, *114*, 1783–1826. (c) Fu, S.; Chen, N. Y.; Liu, X.; Shao, Z.; Luo, S. P.; Liu, Q. Ligand-controlled cobalt-catalyzed transfer hydrogenation of alkynes: Stereodivergent synthesis of Z- and E-alkenes. *J. Am. Chem. Soc.* **2016**, *138*, 8588–8594. (d) Cummings, S. P.; Le, T. N.; Fernandez, G. E.; Quiambao, L. G.; Stokes, B. J. Tetrahydroxydiboron-Mediated Palladium-Catalyzed Transfer Hydrogenation and Deuteriation of Alkenes and Alkynes Using Water as the Stoichiometric H or D Atom Donor. *J. Am. Chem. Soc.* **2016**, *138*, 6107–6110. (e) Espinal-Viguri, M.; Neale, S. E.; Coles, N. T.; Macgregor, S. A.; Webster, R. L. Room Temperature Iron-Catalyzed Transfer Hydrogenation and Regioselective Deuteriation of Carbon-Carbon Double Bonds. *J. Am. Chem. Soc.* **2019**, *141*, 572–582.
- (18) (a) Wang, Y.; Yao, J.; Li, H.; Su, D.; Antonietti, M. Highly selective hydrogenation of phenol and derivatives over a Pd@ carbon nitride catalyst in aqueous media. *J. Am. Chem. Soc.* **2011**, *133*, 2362–2365. (b) Yan, H.; Cheng, H.; Yi, H.; Lin, Y.; Yao, T.; Wang, C.; Li, J.; Wei, S.; Lu, J. Single-atom Pd₁/graphene catalyst achieved by atomic layer deposition: remarkable performance in selective hydrogenation of 1, 3-butadiene. *J. Am. Chem. Soc.* **2015**, *137*, 10484–10487. (c) Upare, P. P.; Lee, J. M.; Hwang, D. W.; Halligudi, S. B.; Hwang, Y. K.; Chang, J. S. Selective hydrogenation of levulinic acid to γ -valerolactone over carbon-supported noble metal catalysts. *J. Ind. Eng. Chem.* **2011**, *17*, 287–292. (d) Hengne, A. M.; Rode, C. V. Cu-ZrO₂ nanocomposite catalyst for selective hydrogenation of levulinic acid and its ester to γ -valerolactone. *Green Chem.* **2012**, *14*, 1064–1072. (e) Liao, F.; Huang, Y.; Ge, J.; Zheng, W.; Tedsree, K.; Collier, P.; Hong, X.; Tsang, S. C. Morphology-Dependent Interactions of ZnO with Cu Nanoparticles at the Materials' Interface in Selective Hydrogenation of CO₂ to CH₃OH. *Angew. Chem., Int. Ed.* **2011**, *50*, 2162–2165.
- (19) An, J.; Farha, O. K.; Hupp, J. T.; Pohl, E.; Yeh, J. I.; Rosi, N. L. Metal-adeninate vertices for the construction of an exceptionally porous metal-organic framework. *Nat. Commun.* **2012**, *3*, 604.